PHILOSOPHICAL TRANSACTIONS OF THE ROYAL SOCIETY A
MATHEMATICAL, PHYSICAL & ENGINEERING SCIENCES

Biologically inspired walking machines: design, control and perception

Rüdiger Dillmann, Jan Albiez, Bernd Gaßmann, Thilo Kerscher and Marius Zöllner

Phil. Trans. R. Soc. A 2007 **365**, doi: 10.1098/rsta.2006.1914, published 15 January 2007

PHILOSOPHICAL TRANSACTIONS OF THE ROYAL SOCIETY A

Phil. Trans. R. Soc. A (2007) **365**, 133–151
doi:10.1098/rsta.2006.1914
Published online 17 November 2006

Biologically inspired walking machines: design, control and perception

By Rüdiger Dillmann*, Jan Albiez, Bernd Gaßmann, Thilo Kerscher and Marius Zöllner

Forschungszentrum Informatik an der Universität Karlsruhe (TH), Interaktive Diagnose und Servicesysteme, Haid-und-Neu-Straße 10-14, 76131 Karlsruhe, Germany

This article presents a set of methods used to support the design and control of biologically inspired walking machines. Starting with a description of the general system design idea, an example for the design of the mechanical construction, a computer supported design procedure for the control architecture and the description of a three-dimensional world model to be used as knowledge base is given. The focus of this paper is on the engineering and integration process and the interrelation between the different phases of the design process.

Keywords: biorobotics; behaviour control; environment models

1. Introduction

Walking robots represent a field of increasing research activity over the last few years. In particular, the ability of walking machines to adapt to unstructured terrain and the resulting requirements to the control architecture are emphasized by the researchers. These efforts can be separated into two different approaches, one being the classical engineering approach using and refining the classical methods of feedback control structures and dynamic modelling to control the robot, e.g. Löffler *et al.* (2001) or Gienger *et al.* (2001). The other way is to adopt as much from biological paragons for locomotion as possible regarding both mechanical design and control architecture, e.g. Ayers *et al.* (2000*a*) and Kimura *et al.* (2001).

Biomechanical research of the last few years has identified several key elements being used in nature for adapting locomotion. These range from the geometrical structure of legs (Witte *et al.* 2001*b*) and dynamic properties of muscles (Pearson 1995) to neural networks used for walking by insects (Cruse & Bartling 1995; Cruse *et al.* 2001). The results of this research imply considerable benefits in case of a transfer of these principles to legged robots. Owing to the high complexity of real walking machines and the impracticality of mimicking, especially nature's actuators and sensors, up to now only some of the ideas have been transferred to the control architectures and design of real robots.

* Author for correspondence (dillmann@ira.uka.de).

One contribution of 15 to a Theme Issue 'Walking machines'.

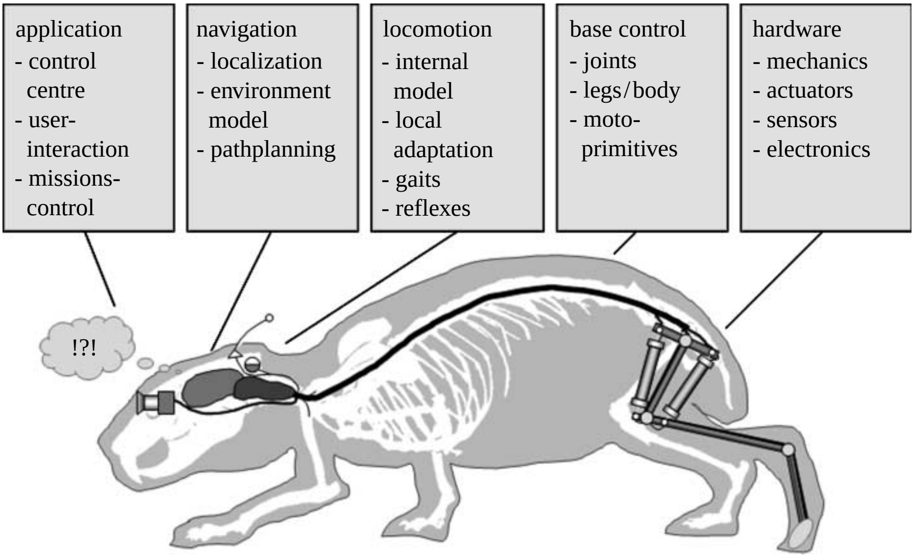

Figure 1. Overview of the different areas of biological inspiration.

The evolutionary selection process influences an animal's morphology, sensors and control system in total. It is not possible nor feasible to copy this process. More interesting is to understand the principles that lead to a problem solution during evolution and to learn from these principles. The main idea of bionics is not to copy nature, but to use the ideas.

In the following, we introduce three main lines of biological inspiration applied to the development of walking robots. Figure 1 shows a detailed overview of each area.

— *Design*. This area covers the mechanical design and actuation of biologically inspired walking robots. We describe how the set-up of the kinematic structure and the choice of the actuators are influenced by the insights of biomechanical research.
— *Control*. Taking the insights of neurobiological research, we propose a new method for behaviour-based control design. This method relies heavily on the structures found in the neural system of animals while using the classical control methods for the implementation of the behaviour units.
— *Perception*. The area of perception focuses on the use of various sensor information to optimize the walking behaviour of the robot. A key element for this system is to use self-reflection to build a feature map of the environment. This map is used to configure the behaviours of the control system.

Since the control system design has to consider the mechanical design characteristics during the construction phase of the robot, and the world model for the robot has to consider the underlying control architecture, each new system characteristic yields to changes in the other areas as well.

Since a robot's hardware is not often changed in comparison with the control software, we study a set of different robot systems, leading to various six- and four-legged walking machines. In this article, we describe three robots: the

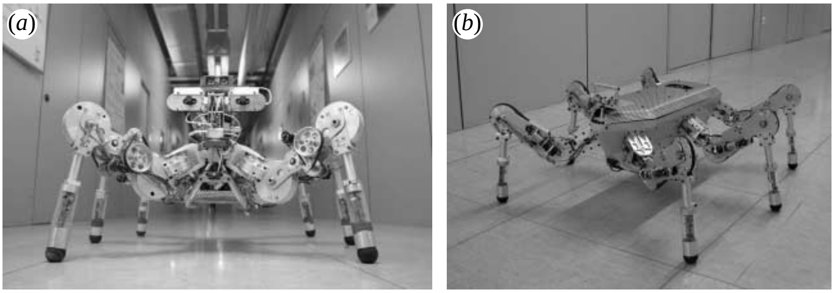

Figure 2. The six-legged, DC-motor actuated walking machines at Forschungszentrum Informatik. (*a*) LAURON III and (*b*) the new LAURON IV.

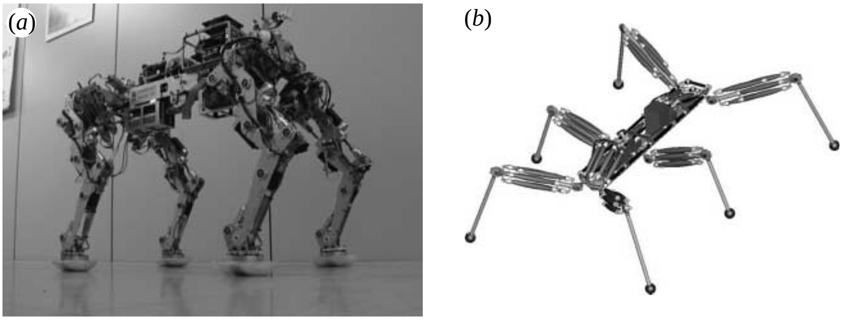

Figure 3. (*a*) The four-legged, DC-motor actuated walking machine BISAM. (*b*) CAD drawing of the six-legged, muscle actuated robot AirINSECT.

four-legged prototype Pneumatically Actuated dyNamically sTable quadrupEd Robot (PANTER) to describe the design principles; the four-legged robot BISAM (figure 3) for introducing the control architecture; and the six-legged robot LAURON III (figure 2) to give an example for the higher perception levels. Considering the age of these systems (PANTER being the newest, LAURON III the oldest robot), one can see how new ideas result in the need of changing the parts it depends on.

2. Design

The morphology of insects and mammals has been optimized by the evolutionary process over the last millenniums. This process results in a quasi-optimal solution for the given purpose. The morphology of animals is highly adapted to the requirements of moving in their habitat. This results in the problem that it is not useful to copy the anatomy of an animal as design rules for walking machines. Definitely, of more interest is the question why the evolutionary selection process resulted in the morphology of the real animal. In this article, we describe the prototype leg of the four-legged mammalian-like robot PANTER (figure 3).

For the design of this robot, we adopted the biological leg parameters of a generalized mammalian leg for the shape and joint configuration; in addition, pneumatically actuated artificial muscles are applied to get a configurable spring–damper system. Recent morphological research has showed that all

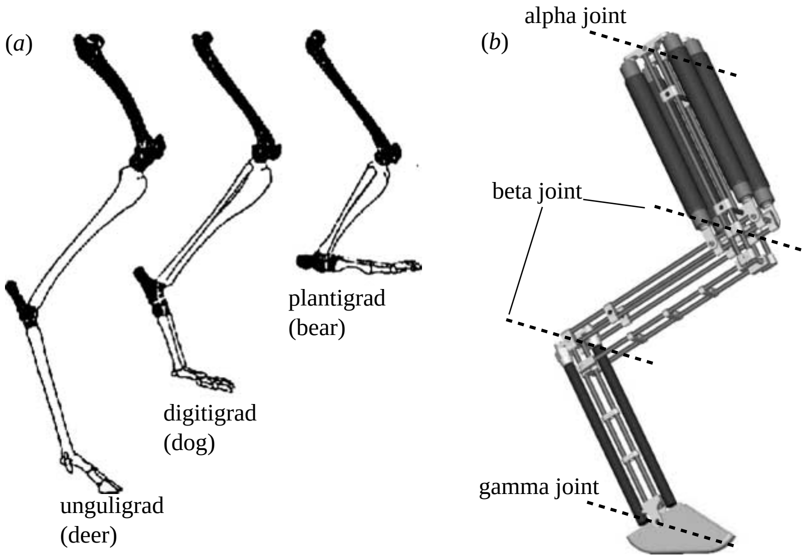

Figure 4. (*a*) Different mammalian leg geometries. (*b*) The revised PANTER leg using carbon-fibre composite, including the joint axes.

mammalian legs share the same basic concept of a z-shaped construction (Witte *et al.* 2001*a*). In figure 4*a*, different leg geometries, as they appear in nature, are shown. The design of the PANTER leg directly reflects this construction (shown in figure 4*b*). The leg consists of three segments equal in length and four active degrees of freedom (d.f.). The distance between the joint axes is 300 mm. The shoulder has two d.f. (α and β). During the power phase, the muscles of the α joint pull the leg backwards and create a forward motion. In the return phase, the leg is pulled to the front of the body. The distance between the shoulder joint and the ground l is significantly influenced by the β joint. Based on the mechanical design, the upper and the lower segments of the leg are held in parallel, which means that $\beta_1=\beta_2$.

The foot has one active d.f., the γ joint. It is used to support the forward motion and acts, like the foot or toes of an animal, as compensation for high changes of angle velocity in the α and β joints during touch-down and lift-off. Earlier designs of the leg had an additional passive d.f., which has been dropped in newer designs owing to the high mechanical complexity. Instead, the foot has a round shape in sagittal direction that ensures an optimal ground contact while abducting the leg.

Figure 5 shows the first functional prototype of this leg. Since this leg is too heavy, a new construction (as shown in figure 4) made of a carbon-fibre composite frame and optimized by finite element modelling simulations has been developed and is currently in construction.

Concerning the behaviour of mammalian legs during running, biomechanical research has shown that the morphology and the spring–damper characteristic of the muscles are key elements of quick locomotion. Evolution has optimized the walking apparatus of mammals to use self-stabilization cycles while running and in case of disturbances, the spring–load of the leg is adapted to stay in these cycles as shown in Geyer *et al.* (2002) and Seyfarth & Geyer (2002).

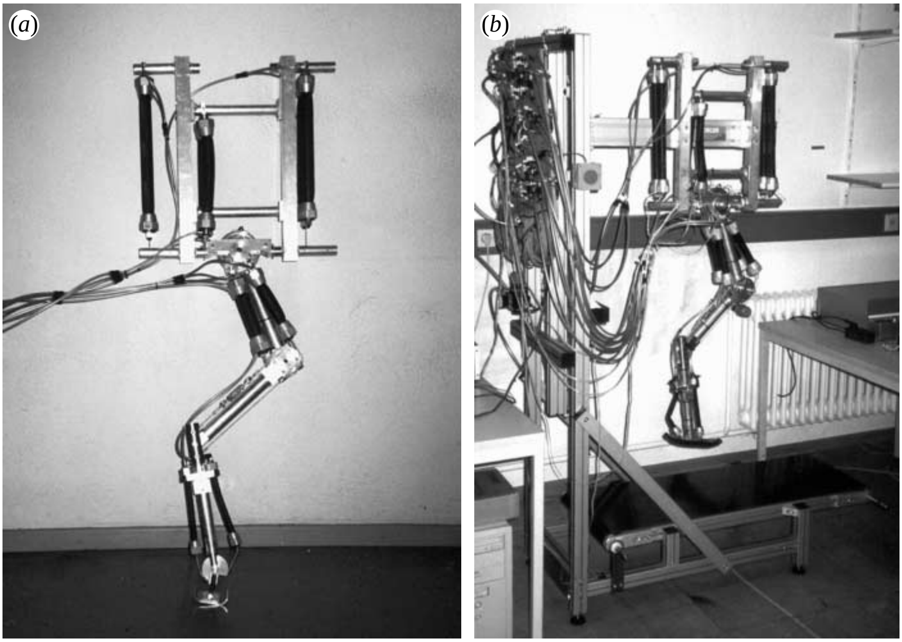

Figure 5. PANTER leg: (*a*) with shoulder fastener and (*b*) muscles test-rig.

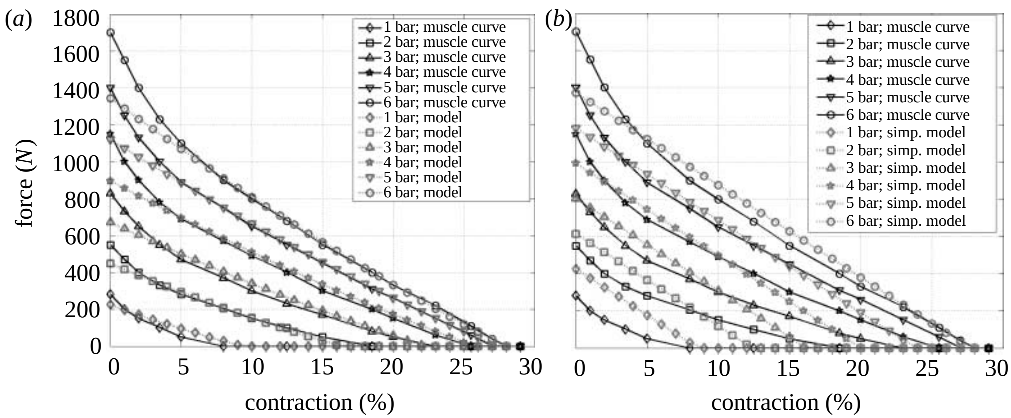

Figure 6. Comparison between muscle model and the real muscle curve. (*a*) Advanced model and (*b*) simplified model.

To achieve this behaviour while using as less closed-loop control as possible, FESTO MAS (FESTO 2003) fluidic muscles are used as actuators. These fluidic muscles are based on the well-known McKibben principle, which is described in Chou & Hannaford (1994) as well as in Tondu & Lopez (2000). The static correlation between contractive force, contraction and pressure of the muscle is shown in figure 6.

The equation describing the static force of the muscle is

$$F_{\text{stat.}}(p,\kappa) = \mu\cdot(\pi r_0^2)\cdot p\cdot(a\cdot(1-\varepsilon(p)\cdot\kappa)^2 - b), \tag{2.1}$$

with the contraction $\kappa = (l_0 - l)/l_0$, the pressure p, the initial muscle radius r_0, the initial fibre angle α_0, the muscle-specific parameters (Tondu & Lopez 2000) $a = 3/\tan^2\alpha_0$ and $b = 1/\sin^2\alpha_0$, the initial length of the muscle l_0, the scalar factor μ, and

$$\varepsilon(p) = a_\varepsilon \mathrm{e}^{-p} - b_\varepsilon. \tag{2.2}$$

The parameters a_ε and b_ε have been found using the least-squares method. Figure 6 presents a comparison between this model and the real muscle curve.

It is necessary to simplify equation (2.1) as the controller should operate on a low-performance micro-controller resulting in

$$F_{\text{mus}}(p, \kappa) = c_1 \cdot p + c_2 \cdot \kappa + c_3. \tag{2.3}$$

The parameter c_i is calculated using the least-squares method. Figure 6 shows the comparison between the simplified model and the real muscle curve. With the help of this simplified model, it is also possible to calculate the pressure, dependent on the force and the contraction,

$$p(F_{\text{mus}}, \kappa) = \frac{F_{\text{mus}} - (c_2 \cdot \kappa) - c_3}{c_1}. \tag{2.4}$$

By applying two of these actuators as antagonistic pairs to a joint, it is possible to configure the stiffness of this joint. A joint position in such a configuration is defined as an equilibrium of the forces exerted by each of the antagonists. Since there is a correlation between length, force and pressure, each joint position can be reached with different overall forces for the same netto force. By configuring the overall force, the stiffness of the joint can be easily controlled by just adjusting the base pressure (see Berns *et al.* 2003).

3. Control

To get an adaptive and stable control of a legged robot, several biologically inspired architectures have been developed in research over the last few decades. In Kimura & Fukuoka (2000) and Kimura *et al.* (2001), a neurooscillator-based pattern generator is introduced. The adaptation to the terrain is solved by directly influencing the activation of the oscillator neurons. Ayers *et al.* (2000*b*) also uses neurooscillators that are parametrized using the results from the analysis of lobsters. Hosoda *et al.* (2000) propose a reflex-based gait generation system, triggered by the input of a camera system mounted on the robot. A distributed control system for a hexapod using reflexes to stabilize the body is presented in Espenschied *et al.* (1996).

Over the last few years, several methods were successfully applied to control the four-legged walking machine BISAM (Berns *et al.* 1998). These include the usage of coupled neurooscillators for gait generation (Ilg *et al.* 1998*a*), learning leg trajectories and the application of radial basis function neural networks and reinforcement learning methods for posture control while trotting (Ilg & Scholl 1998*b*; Albiez *et al.* 2001). All of these methods were successful, but lacked a certain extensibility when confronted with more demands than they were initially designed for (e.g. both dynamically stable trot and statically stable walking). Thus, the necessity arose to build an architecture being able to handle these demands.

We therefore propose a hierarchical built reflex/behaviour network system, which is able to cope with the demands of the control of a walking machine. Behaviour-based architectures have been widely used for the control of mobile robots. The main area of application has been wheel-driven, kinematically extremely simple robots, with the main focus on the robot's task, e.g. navigation and group behaviour (see Mataric 1997; Arkin *et al.* 2000*a*; Endo & Arkin 2001).

There have only been a few attempts to use behaviour-based architectures on the lower levels of the control architecture for kinematically more complex robots like walking machines. The best known and most successful is the subsumption architecture (see Brooks 1986; Ferrell 1995) used on several hexapods. A more biologically inspired approach for a lobster-like robot is proposed in Ayers *et al.* (2000*a*). But there are several drawbacks to these architectures, among them is a general tendency towards scalability problems; weaknesses when adding new behaviours or trying reusing the existing ones; and in most cases a highly problem-specific approach (see Arkin 2000*b*).

(*a*) *Motivation*

When considering the insights gained through PET and EEG scans and spinal cord activity plots of animals performing certain tasks (Pearson 1995; Kandel *et al.* 2000), as well as the problems when dealing with real sensor information and highly complex robots, the following key aspects can be identified.

- A certain action of an animal always creates activity in the same area of the animal's brain or its spinal cord.
- Such an active area can result in the stimulation of further regions as well as inhibit activity in others.
- Even though the classical approach to robot control has difficulties in handling the complexity of the whole system, these established methods should be applied to solve simpler sub-problems.
- As hierarchical systems have been approved in robotics as well as in nature, it is advisable to use some kind of levelled system with an increasing degree of abstraction regarding sensor data and motor signals.

Taking these observations into consideration, we designed a control architecture consisting of a hierarchical network of behaviours. Each behaviour or reflex[1] is developed using methods of classical control system design or artificial intelligence. Only the interaction of the behaviours and their placement in the network will result in the desired actions of the overall system.

(*b*) *Behaviours*

A behaviour or reflex $\mathcal{B}$ in the sense of this architecture is a functional unit that generates an output vector $\boldsymbol{u}$ using an input vector $\boldsymbol{e}$ and an activation ι according to a transfer function $F(\boldsymbol{e})$. Additionally, a target rating criterion $r(\boldsymbol{e})$ and a behaviour activity a are calculated. Mathematically, this can be

[1] A reflex refers to a simple behaviour close to the hardware, thus being more reactive than deliberative.

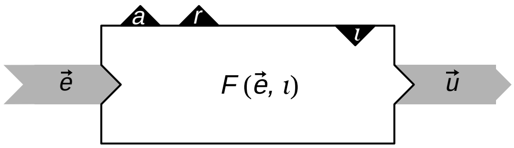

Figure 7. Behaviour design.

combined with the 6-tuple

$$\mathcal{B} = (\boldsymbol{e}, \boldsymbol{u}, \iota, F, r, a).$$

The transfer function F is defined as in equation (3.1) for an input dimension of n and an output dimension of m. It implements the fundamental action being performed by the behaviour. The output vector $\boldsymbol{u}$ is generated in two steps. First, an unmodified output with respect to the input vector $\boldsymbol{e}$ is produced. In the second step, this output is modified according to the activation ι. Generally speaking, an ι of 0 means that the behaviour will generate no output at all, one of 1 will lead to the full output. For simple behaviours, for example posture control reflexes implemented by a classical controller, the output is scaled between 0 and 1. In more deliberative behaviours, like the swing or a gait behaviour, ι could express an increasing tendency to perform an action (figure 7),

$$F : \Re^n \times [0;1] \rightarrow \Re^m; \quad F(\boldsymbol{e}, \iota) = \boldsymbol{u}. \tag{3.1}$$

This activation mechanism ensures the robot's safety to a certain degree by activating only a defined set of behaviours and enables the usage of the behaviour as an abstract actor by other higher level behaviours.

While the formal definition above is an abstract view of the behaviour, the actual implementation method can vary from simple feedforward controllers up to more complicated systems like finite state automata or algorithms used in artificial intelligence.

As mentioned above, each behaviour generates a target rating r, defined in equation (3.2), evaluating how far the actual state of the robot matches the aspired goal of the behaviour. For this estimation, the input vector $\boldsymbol{e}$ consisting of sensor information from the robot and outputs of other behaviours is used. A value of 0 indicates that the robot's state matches the behaviour's goal, but a value of 1 indicates that it does not. It is constantly updated even if the behaviour is deactivated and generates no output,

$$r : \Re^n \rightarrow [0;1]; \quad r(\boldsymbol{e}) = r. \tag{3.2}$$

For monitoring reasons, it is desirable to have some visualization of the behaviour's activity. But even more importantly, the activity is used as feedback information for other behaviours and for behaviour coordination. The activity a is defined in equation (3.3). Colloquial a can be interpreted as an indication on the behaviour's effort in transferring the robot to a state achieving its goal,

$$a : \Re^m \rightarrow [0;1] : a(\boldsymbol{u}) \sim \|\boldsymbol{u}\|. \tag{3.3}$$

(c) *Behaviour coordination*

Following the approach of Brook's subsumption architecture, the behaviours are placed on layers depending on how much they actually work on the robot's hardware. The inputs and outputs of each behaviour are connected with each

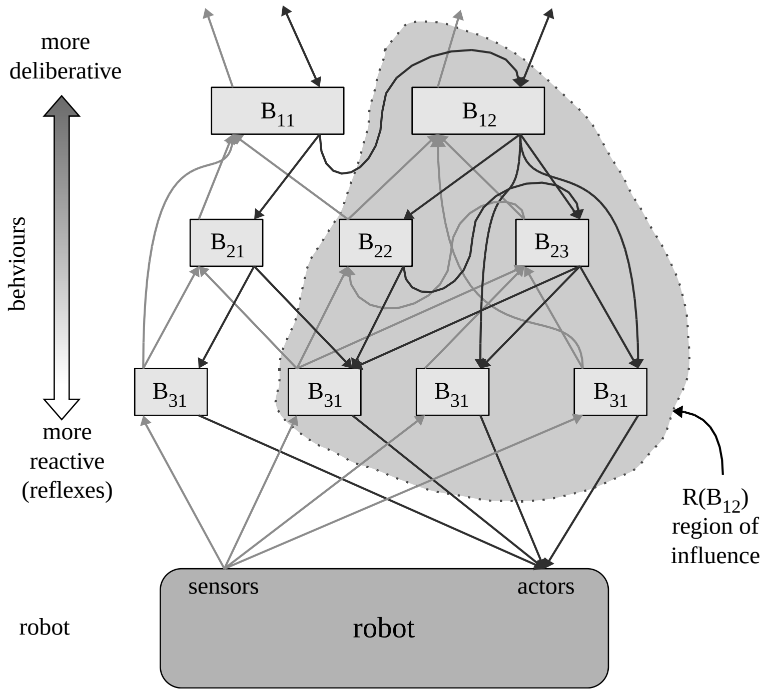

Figure 8. Behaviour coordination network.

other to form a network structure (see figure 8 for an example). These connections transport control and sensor information as well as loop-back information like r, ι and a of different behaviours. In case several outputs of different behaviours are connected to the same input of another behaviour, a behaviour activity-based fusion scheme is used (figure 9). This scheme favours the output of behaviours having an unmet target (i.e. a high r) and a high activity a implying a ι greater than 0. The actual fusion of the outputs is done with the help of a fusion knot. Basically, a fusion knot is no more than a fusion function f combining the outputs $\boldsymbol{u}$, the activities a and the target ratings r of all behaviours involved to generate one output vector $\boldsymbol{u}'$,

$$f : \Re^n \times \cdots \times \Re^n \times \Re \times \cdot\cdot \Re \rightarrow \Re^n : f(\boldsymbol{u}_0, \ldots, \boldsymbol{u}_n, a_0, \ldots, a_n, r_0, \ldots, r_n) = \boldsymbol{u}'. \tag{3.4}$$

In most cases, either only the output of the behaviour with the highest activity (winner takes it all) is used or the average of all outputs weighted by the activities is calculated by f. However, it is possible to implement even more complex fusion schemes if it is necessary. This allows the usage of the behaviours' activity a and target rating r as a mean for behaviour coordination without directly using the values of the actual control data generated by the behaviour. This way the output fusion is independent of the scaling of the control data and it is ensured that two behaviours competing over the influence on another behaviour will not annihilate each other's output. This fusion scheme can be positioned between fuzzy and multiple objective behaviour coordination (see Pirajanian 1999).

The activity in such a network will concentrate inside the influence area or region $\mathcal{R}$ of a higher level behaviour. $\mathcal{R}$ is recursively defined as in equation (3.5),

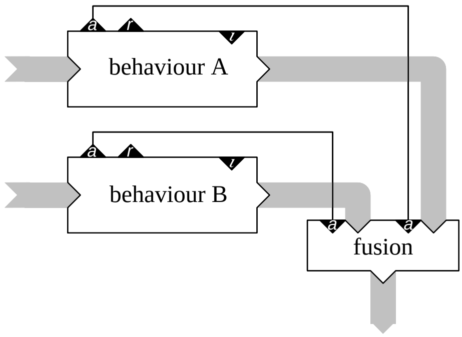

Figure 9. The general fusion scheme.

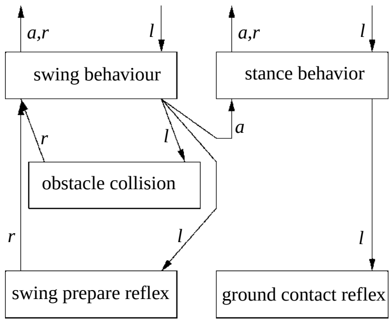

Figure 10. Behaviour network for one leg.

where $\mathrm{Act}(B)$ is the set of behaviours being influenced by $\mathcal{B}$ via ι,

$$\mathcal{R}(B) = \bigcup_{B_i \in \mathrm{Act}(B)} \{B_i \cup \mathcal{R}(B_i)\},$$

$$\mathcal{R}(B) = 0, \quad \text{if } \mathrm{Act}(B) = 0. \tag{3.5}$$

A region is an organizational unit of cooperating behaviours. The affiliation of a behaviour to a region is not exclusive. For example, a leg's swing behaviour is located in the region of a stride and a trot behaviour. To coordinate the influence of several high-level behaviours on a lower one, a fusion knot is inserted before its ι input. An example for the coordination of the influence of two behaviours on a third is shown in figure 9.

Figure 10 shows the behaviour network belonging to a leg as an example for a behaviour network. Note that the stance behaviour is inhibited by the swing behaviour via the activity, and such guaranteeing, that stancing will stop as soon as the leg is cleared for swinging. The two 'helper' behaviours, preparing a swing phase and keeping the ground contact, are the most reactive in this group and as such are placed at the bottom.

— *Swing*. This behaviour calculates the swing trajectory for a leg. When activated, it waits until the lower reflexes signal that the weight of the robot is removed from the leg. When this is accomplished, a swing trajectory for the leg is calculated and executed. As long as the swing is in progress, the activity of this behaviour inhibits the stance behaviour.

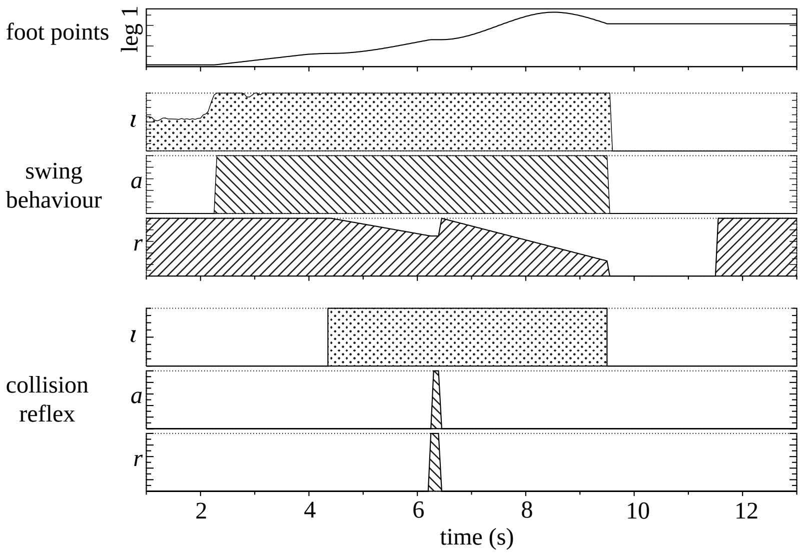

Figure 11. Some behaviours when colliding with an obstacle.

— *Stance*. The leg is pushed in the opposite direction of the robot resulting in a forward movement. This behaviour is switched off as long as there is an activity from the swing behaviour and activates its helper *ground contact*.

— *Obstacle collision*. This reflex monitors the force sensors in the foot and detects a collision with an obstacle. When this happens, the foot is pulled away from the obstacle and the swing behaviour is reset.

The reaction of the control architecture when BISAM hits an obstacle during the swing phase is presented in figure 11. This experiment shows the reaction of the robot when the swing leg collides with a higher obstacle or fails to make contact with the ground after the swing is finished. In the latter case, the robot will search for ground by stretching the leg and lowering the body, and repositioning the foot when unsuccessful. The former case is shown in figure 11; the leg swing is represented by the z-position of the foot point and the swing behaviour is plotted as well. As soon as the foot collides with the obstacle (note the peak is at approx. $t = 6$ s), the collision reflex reacts, being activated by the swing behaviour since the foot left the ground. The foot is pulled back and the collision is resolved. The peak of the reflex's target rating serves as signal for the swing behaviour, which will start a new swing from the actual foot point to a raised target point. The resulting foot point trajectory is shown in figure 12.

To allow the transition of the activity between different regions, r and a are loop-backed between behaviours on the same level as well as on others. This way it is possible that at a point where one behaviour cannot handle a situation anymore even when it is fully in charge, another behaviour that can solve the situation is activated while the first behaviour is deactivated. If, for example, the desired speed of a walking machine cannot be achieved, a gait change is initiated (as shown in Albiez *et al.* 2003).

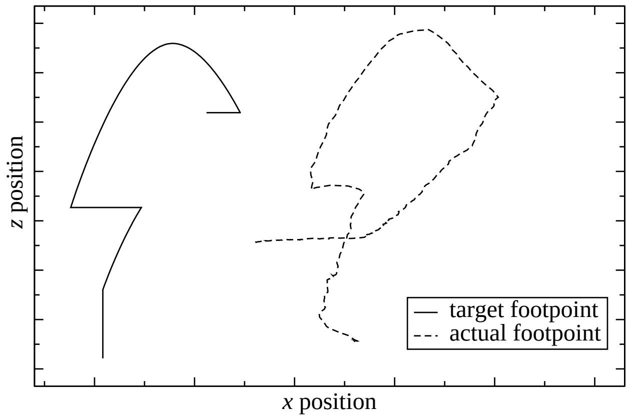

Figure 12. Trajectory of the foot point in case of an obstacle collision.

4. Perception

To actually use the flexibility of legged systems, there has to be a certain amount of knowledge of the environment around the robot. Using only the 'pure' reflex architecture results in a low speed on irregular terrain. The robot tends to make mistakes (e.g. hitting an obstacle with every leg) over and over again, since the reflexes and low-level behaviour are not able to learn anything about their environment. To compensate these problems, a perception layer has to be designed. For this, it is necessary to have a three-dimensional model of the robot's adjacent environment that acts as a knowledge base for activating the correct behaviours for traversing it. The first steps for realizing such a model are implemented on LAURON III (Gaßmann *et al.* 2001), which features a relative robust control architecture and, being a six-legged system, is more robust to irregular terrain. Since we are at the beginning of this work, the lower speed of a six-legged machine in this case is not considered a drawback.

Much work concerning three-dimensional environment models has already been done, but it mostly focuses on wheel-driven vehicles (e.g. Stuck *et al.* 1994; Kruse *et al.* 1996; Murphy *et al.* 2002). All of these use some sort of *occupancy grid* (Elfes 1989) for representation, which proved to be very effective, but none of these approaches considers the specific needs of a walking robot. Since legged machines are supposed to overcome obstacles instead of just avoiding them, the placement of the feet during walking is an important task to be considered when designing the environment model. Some huge walking robots, like the ADAPTIVE SUSPENSION VEHICLE (Bihari *et al.* 1989), the AMBLER (Wettergreen *et al.* 1990), or the DANTE II (Bares & Wettergreen 1999), were able to build local elevation maps by using huge and heavy three-dimensional distance laser sensors. Smaller machines like LAURON III have to generate the map step-by-step on the basis of sparse sensory information, which moreover requires the accurate determination of the robot's spatial position and orientation to guarantee a consistent and thus useable map of the environment.

(*a*) *The localization task*

Outdoor localization of mobile robots in general is a challenging task. The robot moves in rough terrain with an unstructured surrounding and changing light conditions. Maps of the environment are rarely available, so that localization via the detection of well-known landmarks is hardly possible. In general, the complexity of landmark and/or map-based localization algorithms increase tremendously in an outdoor application. The fact that the algorithms have to run on board of a middle-sized autonomous walking robot complicates the situation even more. The body of a walking robot is capable of moving in an omnidirectional way with six d.f.. Since the load of such a walking robot is very restricted, there are further limitations on the sensor system and the computational power able to cope with this.

Following existing outdoor localization approaches (e.g. Fuke & Krotkov 1996; Goel *et al.* 1999 or Sukkarieh *et al.* 1999), one can state that the combination of several different localization methods is strongly indicated. Our proposed approach uses the robot's odometry calculation as the permanent available, basic relative measuring method. Absolute position and orientation information is fused to restrict the localization error by using a Kalman filter. A GPS receiver seems to be applicable for the correction of the global position, especially if one thinks about the availability of a satellite-based differential GPS[2]. Information about the absolute spatial orientation of the robot could be gained by the use of accelerometers detecting the direction of gravity in combination with magnetometers to know the direction of the geographical north.

The calculation of the walking robot odometry is based on the solution presented by Roston & Krotkov (1992). Unlike AMBLER, which moved only one leg at a particular time, LAURON III in general swings multiple legs simultaneously. Respecting the robot dimension, the walking speed of LAURON III is also much higher. In unstructured terrain, this often leads to partially slipping feet in the support phase, so that the classification of *slipping fe*et and *not slipping feet* is not obvious any more. Therefore, we propose a preliminary fuzzy reasoning step to generate a fine granular weight factor for each leg (figure 13*a*). In the first stage, the leg states *ground contact*, *slipping* and *collision* $\in[0;1]$ are rated from sensor measurements like contact forces, joint angles and motor currents. The second stage then evaluates the overall weight $\in[0;1]$, which is passed to the odometry calculation.

Figure 13*b* illustrates a schematic of the proposed feedback error state Kalman filter to correct the position and orientation errors. Contrary to the odometry of wheel-driven mobile robots, the odometry calculation of walking robots itself is too complex to serve as a system model for the filter. Taking the relative character of the odometry into account, we propose to present the velocities and the angular velocities in the robot coordinate system to the Kalman filter. The derivation of the filter model then could be adapted from an INS/GPS coupling Kalman filter (Gaßmann *et al.* 2005).

[2] EGNOS, European Geostationary Navigation Overlay System; WAAS, Wide Area Augmentation System in North America.

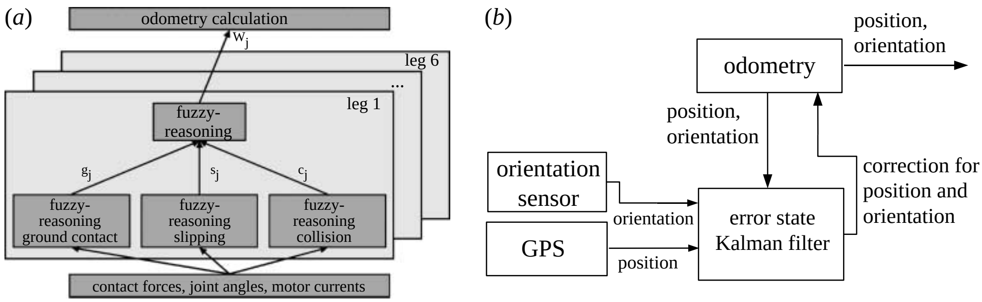

Figure 13. Robot localization. (*a*) Odometry calculation with preliminary fuzzy reasoning step. (*b*) Schematic of the feedback error state Kalman filter.

(*b*) *The mapping task*

Navigation in unstructured, mostly unknown, terrain implies some restrictions to the representation of the environment. The required representation method should be independent of edge detection, because no edges can be expected in a natural environment. In order to place the feet at proper locations, the resolution of the maps must be high and exact, especially in the direct surroundings of the machine. Taking these aspects into account yields to a geometric representation approach for mapping the environment. Small robots are not able to carry large numbers of sensors. Thus, map generation has to be done on the basis of sparse sensory information. To handle white areas with insufficient environment data, the robot should be able to provide the mapping module with additional measurements.

Comparing existing mapping approaches for walking machines, we found the *occupancy grid* method (Elfes 1989) very suitable. Our proposed approach, the *advanced inference grid*, is a variant of the *vector field histogram* method (Borenstein & Koren 1991). Out of each measurement (which can be achieved by a distance laser sensor or tactile feet), the global coordinates of the hit voxel and the corresponding grid cell are calculated, and its content is modified. For the distance sensor, all the cells lying on a straight line between the detected cell and the one corresponding to the robot's head position, which are obviously empty, are also regarded. In our approach, the content of each cell does not consist only of an occupancy value, but a *credibility* value is also stored. Both values range from 0 to 1. The occupancy value occ(C) reveals the occupancy state of the area represented by the grid cell C—insofar as it is known. The credibility value cred(C) states how much we are able to trust this observation. This division is done for the following purpose. We want to distinguish whether a stored occupancy of, for example, 0.5 indicates a fairly correct observation of an inhomogeneous environment or just measurements of improper quality, a drawback that, if detected, can be repaired easily by invoking additional measurements or, alternatively, a more cautious walking behaviour of the robot.

In addition, a grid cell stores further meta data to support the update of the cell content, e.g. total amount of measurements, age of the latest measurement and number of different contributed sensors. Figure 14 illustrates the data flow on updating a grid cell C when new sensor data are available. A parameter estimation based on fuzzy reasoning determines the credibility of the

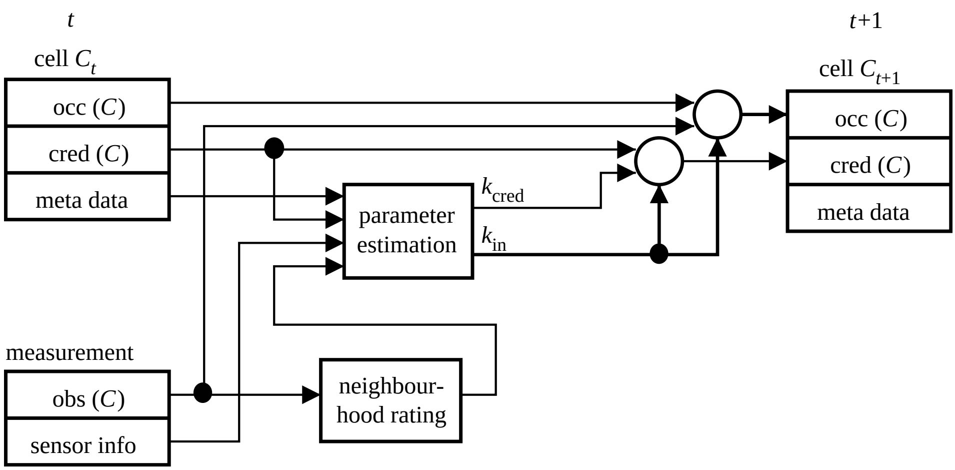

Figure 14. Schematic of data flow and interaction while integrating new sensor measurements into a grid cell C.

measurement $k_{\text{cred}} \in [0,1]$ and the influence of the measurement on the cell content $k_{\text{in}} \in [0,1]$. With $\text{obs}(C_t) \in \{0,1\}$ being the actual observation, the new cell content calculates

$$\begin{aligned} \text{occ}(C_{t+1}) &= (1-k_{\text{in}})\cdot\text{occ}(C_t) + k_{\text{in}}\cdot\text{obs}(C_t), \\ \text{cred}(C_{t+1}) &= (1-k_{\text{in}})\cdot\text{cred}(C_t) + k_{\text{in}}\cdot k_{\text{cred}}. \end{aligned} \tag{4.1}$$

The fuzzy rules allow an easy and fast method for filtering the incoming sensor data, e.g. if there were many measurements so far, the influence of the sole actual measurement is low. If the latest measurement is rather old, the influence of the actual measurement is high. If the grid cells in the neighbourhood reflect the actual observation, the measurement credibility k_{cred} is high. The use of this meta information is one of the main differences from the vector field histogram, the influence of each measurement is dependent on the quality of both prior and actual data. Averaged information will be easily erased out of the model, new and good observations will have greater influence than redundant weak-quality information.

(*c*) *The adaptation task*

Storing three-dimensional data results in a need for a huge amount of memory, even though octrees are used for representing the map contents. Furthermore, planning in a three-dimensional map is computationally extremely expensive. In order to save memory and gain processing efficiency, the three-dimensional base map only contains the immediate surrounding of the walking robot and scrolls as the machine is moving. A global two-dimensional elevation map for further processing is generated by projection (figure 15).

One of the most relevant decisions for a walking machine is the selection of the footprints. Each time before the execution of a new step is invoked, the expected next footprint is calculated assuming an even and flat ground. Using the two-dimensional elevation map, the target area is searched for the most credible

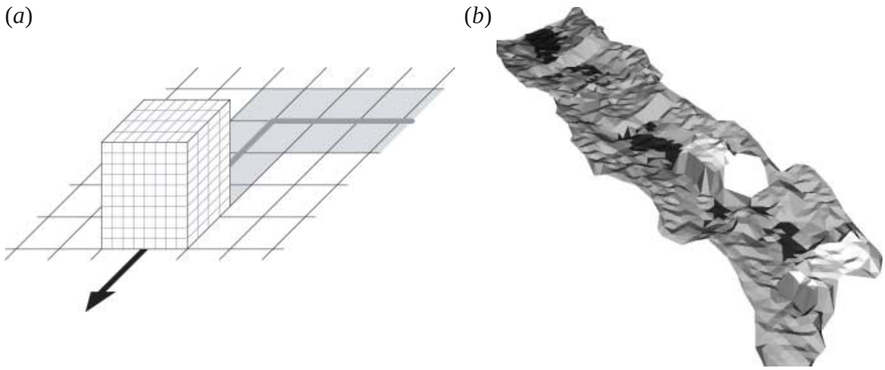

Figure 15. Map generation. (*a*) The local three-dimensional map scrolls with the moving robot. (*b*) The two-dimensional global elevation map is generated by projection.

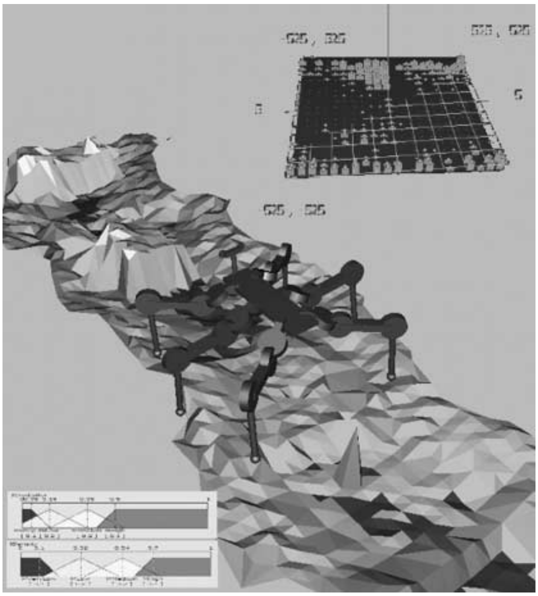

Figure 16. A model of the walking machine upon the elevation map. In the upper right corner the *roughness* of the map is illustrated, the lower left corner denotes the fuzzy-based rating.

location, which can be expected to be a secure place for the robot's foot (Gaßmann *et al.* 2003). Finally, that footprint is passed to the walking control module. This enables the machine to perform planned steps on elevations or into slots without collisions (which for example invoke the elevator reflex) or search for ground and therefore accomplish a fluid motion.

Looking ahead even further, several geometrical parameters describing the near environment are extracted from the two-dimensional elevation map like *inclination*, *roughness* or *average obstacle size*. In addition, non-geometrical attributes like *ground softness* are stored while walking on the terrain (figure 16). These data are applied to a fuzzy-based rating, deciding on general walking parameters like *velocity*, *gait*, *step-height* and *inclination-mode*.

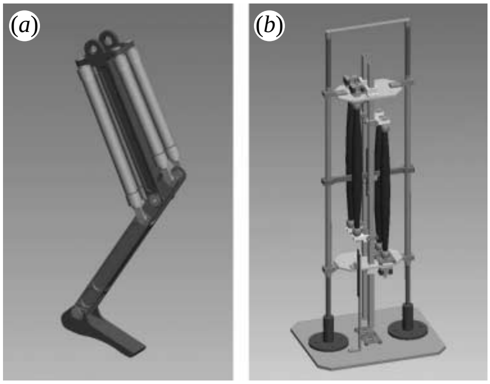

Fig. 17. Prototypes of the two-legged robot project. (*a*) Study of a single leg. (*b*) Two-legged-muscle test and integration environment.

5. Conclusion and outlook

In this article, a design philosophy for designing and controlling biologically inspired walking machines was presented. As examples for the mechanical design, the prototype leg for a mammalian-like four-legged walking machine was introduced. As actuators, pneumatic artificial muscles are used to model the spring–damper characteristics of the biological muscles. As a control method, we presented a behaviour network architecture and a method to map and classify the environment around a walking machine and used this information for behaviour selection.

Future work will consist of implementing the world model and the control architecture on the newer systems, which actually means that the design cycle will be closed again. In detail, this will consist of using the three-dimensional world model for a very adaptive free-gait and trot for the four-legged machine BISAM. The behaviour networks are currently implemented on the six-legged robot LAURON III, and a system to integrate the world model and the behaviour architecture more tightly is in development. Moreover, a path planner for walking machines on the basis of the two-dimensional elevation map is in test stage.

Currently, we have started a new project to design a two-legged robot with an adjustable spring–damper system in the knees (figure 17). In this project, we will combine the experience made with the introduced robots in one walking robot. Especially in the areas of actuation and control, we will use the presented methods to transfer biomechanical and neurobiological expertise to engineering.

The authors would like to thank the German Research Foundation (DFG) for sponsoring their work over the last years.

References

Albiez, J., Ilg, W., Luksch, T., Berns, K. & Dillmann, R. 2001 Learning reactive posture control on the four-legged walking machine bisam. In *Proc. Int. Conf. on Intelligent Robots and Systems (IROS), Hawaii, USA.*

Albiez, J., Luksch, T., Berns, K. & Dillmann, R. 2003 An activation-based behaviour control architecture for walking machines. *Int. J. Robot. Res.* **22**, 203–211. (doi:10.1177/0278364903022003005)

Arkin, R., Kahled, A., Weitzenfeld, A. & Cervantes-Prez, F. 2000*a* Behavioral models of the praying mantis as a basis for robotic behavior. *J. Auton. Syst.* **32**, 39–60. (doi:10.1016/S0921-8890(99)00121-9)

Arkin, R. 2000*b* *Behavior-based robotics.* Cambridge, MA: MIT Press.

Ayers, J., Witting, J., Olcott, C., McGruer, N. & Massa, D. 2000*a* Lobster robots. In *Proc. Int. Symp. on Aqua Biomechanisms.*

Ayers, J., Witting, J., Wilbur, C., Zavracky, P., McGruer, N. & Massa, D. 2000*b* Biomimetic robots for shallow water mine countermeasures. In *Proc. Autonomous Vehicles in Mine Countermeasures Symp.*

Bares, J. E. & Wettergreen, D. S. 1999 Dante II: technical description, results, and lessons learned. *Int. J. Robot. Res.* **18**, 621–649. (doi:10.1177/02783649922066475)

Berns, K., Ilg, W., Eckert, M. & Dillmann, R. 1998 Mechanical construction and computer architecture of the four-legged walking machine bisam. In *Proc. 1st Int. Conf. Climbing and Walking Robots (CLAWAR), Brussels, Belgium*, pp. 167–172.

Berns, K., Kerscher, T., Albiez, J., Grimminger, F. & Hochholdinger, U. 2003 Design and control of a leg for the running machine panter. In *Proc. Int. IEEE Conf. on Advanced Robotics, Coimbra, Portugal.*

Bihari, T., Walliser, T. & Paterson, M. 1989 Controlling the adaptive suspension vehicle. *Computer* **22**, 59–65. (doi:10.1109/2.30721)

Borenstein, J. & Koren, Y. 1991 The vector field histogram—fast obstacle avoidance for mobile robots. *IEEE Trans. Robot. Automat.* **7**, 278–288. (doi:10.1109/70.88137)

Brooks, R. 1986 A robust layered control system for a mobile robot. *IEEE J. Robot. Automat.* **2**, 14–23.

Chou, C. P. & Hannaford, B. 1994 Static and dynamic characteristics of McKibben pneumatic artificial muscles. *Int. Conf. Robot. Automat.* **1**, 281–286.

Cruse, H. & Bartling, C. 1995 Movement of joint angles in the legs of a walking insect, *Carausius morosus. J. Insect Physiol.* **41**, 761–771. (doi:10.1016/0022-1910(95)00032-P)

Cruse, H., Dürr, V. & Schmitz, J. 2001 Control of a hexapod walking—a decentralized solution based on biological data. In *Proc. 4th International Conference on Climbing and Walking Robots (CLAWAR), Karlsruhe, Germany.*

Elfes, A. 1989 Using occupancy grids for mobile robot perception and navigation. *Computer* **22**, 46–57. (doi:10.1109/2.30720)

Endo, Y. & Arkin, R. 2001 Implementing Tolman's schematic sowbug: behaviour-based robotics in the 1930s. In *Proc. 2001 IEEE Int. Conf. on Robotics and Autonomous Systems.*

Espenschied, K., Quinn, R., Chiel, H. & Beer, R. 1996 Biologically-based distributed control and local reflexes to improve rough terrain locomotion in a hexapod robot. *Robot. Auton. Syst.* **18**, 59–64. (doi:10.1016/0921-8890(96)00003-6)

Ferrell, C. 1995 Global behavior via cooperative local control. *Automon. Robots* **2**, 105–125. (doi:10.1007/BF00735430)

FESTO 2003 Pneumatic Catalogue 2003—Pneumatic drives. http://www.festo.com.

Fuke, Y. & Krotkov E. 1996 Dead reckoning for a lunar rover on uneven terrain. In *Proc. IEEE Int. Conf. on Robotics and Automation*, pp. 411–416.

Gaßmann, B., Scholl, K. & Berns, K. 2001 Locomotion of LAURON III in rough terrain. In *Proc. Int. Conf. on Advanced Intelligent Mechatronics, Como, Italy*, pp. 959–964.

Gaßmann, B., Frommberger, L., Dillmann, R., Berns, K. 2003 Real-time 3D map building for local navigation of a walking robot in unstructured terrain. In *Proc. IEEE/RSJ Int. Conf. on Intelligent Robots and Systems, Las Vegas, USA*, pp. 2185–2190.

Gaßmann, B., Zacharias, F., Zöllner, J. M. & Dillmann, R. 2005 Localization of walking robots. In *Proc. IEEE Int. Conf. on Robotics and Automation (ICRA), Barcelona, Spain.*

Geyer, H., Seyfarth, A. & Blickhan, R. 2002 Natural dynamics of spring-like running—emergence of self-stability. In *5th Int. Conf. on Climbing and Walking Robots (CLAWAR), Paris, France.*

Gienger, M., Löffler, K. & Pfeiffer F. 2001 In *Proc. IEEE Int. Conf. on Robotics and Automation (ICRA).*

Goel, P., Roumeliotis, S. I. & Sukhatme, G. S. 1999 Robust localization using relative and absolute position estimates. In *Proc. IEEE Int. Conf. on Intelligent Robots and Systems*, pp. 1134–1140.

Hosoda, K., Miyashita, T. & Asada, M. 2000 Emergence of quadruped walk by a combination of reflexes. In *Proc Int. Symp. on adaptive Motion of Animals and Machines, Montreal, Canada.*

Ilg, W., Albiez, J. & Jedele, H. 1998*a* A biologically inspired adaptive control architecture based on neural networks for a four-legged walking machine. In *Proc. 8th Int. Conf. on Artificial Neural Networks, Skoevde, Sweden*, pp. 455–460.

Ilg, W. & Scholl, K.-U. 1998*b* Cqran: continuous q-learning resource allocation network. Towards reinforcement learning with multi-dimensional continuous action spaces. In *Proc. 8th Int. Conf. on Artificial Neural Networks, Skoevde, Sweden*, pp. 455–460.

Kandel, E., Schwartz, J. & Jessel, T. M. 2000 *Principles of neural science*, 4th edn. New York, NY: McGraw-Hill.

Kimura, H. & Fukuoka, Y. 2000 Biologically inspired dynamic walking on irregular terrain—adaptation at spinal cord and brain stem. In *Proc. Int. Symp. on Adaptive Motion of Animals and Machines, Montreal, Canada.*

Kimura, H., Fukuoka, Y., Hada, Y. & Takase, K. 2001 Three-dimensional adpative dynamic walking of a quadruped robot by using neural system model. In *Proc. 4th Int. Conf. on Climbing and Walking Robots (CLAWAR), Karlsruhe, Germany.*

Kruse, E., Gutsche, R. & Wahl, F. M. 1996 Efficient, iterative, sensor based 3-D map building using rating functions in configuration space. In *Proc. IEEE Intelligent Conf. on Robotics and Automation, Minneapolis, Minnesota, vol. 2*, pp. 1067–1072.

Löffler, K., Gienger, M. & Pfeiffer, F. 2001 Simulation and control of a biped jogging robot. In *Proc. 4th Int. Conf. on Climbing and Walking Robots (CLAWAR), Karlsruhe, Germany.*

Mataric, M. J. 1997 Behavior-based control: examples from navigation, learning, and group behavior. *J. Exp. Theor. Artif. Intell.* **9**, 323–336.

Murphy, K., Abrams, M., Balakirsky, S., Chang, T., Hong, T., Lacaze, A. & Legowik, S. 2002 Intelligent control for off-road driving. In *First Int. NAISO Congress on Autonomous Intelligent System* (ed. S. Nahavandi), Natural and Artificial Intelligence Systems Organization.

Pearson, K. 1995 Proprioceptive regulation of locomotion. *Curr. Opin. Neurobiol.* **5**, 768–791. (doi:10.1016/0959-4388(95)80107-3)

Pirajanian, P. 1999 Behaviour coordination mechanisms—state-of-the-art. Technical Report IRIS-99-375, Institute for Robotics and Intelligent Systems, School of Engineering, University of Southern California.

Roston, G. P. & Krotkov, E. P. 1992 Dead reckoning navigation for walking robots. In *Proc. IEEE/RSJ Int. Conf. on Intelligent Robots and Systems, Raleigh, NC, USA*, pp. 607–612.

Seyfarth, A. & Geyer, H. 2002 Natural control of spring-like running—optimzed self-stabilization. In *Proc. 5th Int. Conf. on Climbing and Walking Robots (CLAWAR), Paris, France.*

Stuck, E., Manz, A., Green, D. A. & Elgazzar, S. 1994 Map updating and path planning for real-time mobile robot navigation. In *Proc. IEEE Int. Conf. on Intelligent Robots and Systems, Munich, Germany*, pp. 753–760.

Sukkarieh, S., Nebot, E. & Durrant-Whyte, H. F. 1999 A high integrity imu/gps navigation loop for autonomous land vehicle applications. In *IEEE Trans. Robot. Automation*, *vol. 15*, pp. 571–578.

Tondu, B. & Lopez, P. 2000 Modeling and control of McKibben artificial muscle robot actuators. *IEEE Control Syst. Mag.* **20**, 15–38. (doi:10.1109/37.833638)

Wettergreen, D., Thomas, H. & Thorpe, C. 1990 Planning strategies for the ambler walking robot. In *Proc. IEEE Int. Conf. on Systems Engineering*, pp. 198–203.

Witte, H., Hackert, R., Fischer, M. S., Ilg, W., Albiez, J., Dillmann, R. & Seyfarth, A. 2001*a* Design criteria for the leg of a walking machine derived by biological inspiration from quadruped mammals. In *Proc. 4th Int. Conf. on Climbing and Walking Robots (CLAWAR), Karlsruhe, Germany.*

Witte, H. *et al.* 2001*b* Transfer of biological priciples into the construction of quadruped walking machines. In *Proc. Second Int. Workshop On Robot Motion And Control, Bukowy Dworek, Poland.*